Journal of Catalysis **184,** 172–179 (1999)
Article ID jcat.1999.2430, available online at http://www.idealibrary.com on IDEAL®

Low-Temperature CO Adsorption on V-Containing Aluminophosphates: An FTIR Study

Patricia Concepción,[1] Konstantin Hadjiivanov,[2] and Helmut Knözinger[3]

Institut für physikalishe Chemie, Univeristät München, Sophienstr. 11, 80333 München, Germany

Received October 6, 1998; revised January 13, 1999; accepted January 14, 1999

Adsorption of CO on VAPO-5 and VMgAPO-5 has been studied by IR spectroscopy. No carbonyl species were formed with V^{5+} sites on oxidized VAPO-5. Mild reduction (673 K) of the sample with hydrogen generated V^{4+} sites which did not form stable complexes with CO at ambient temperature. At 85 K, however, two V^{4+}–CO species were detected, characterized by bands at 2200 (A species) and 2194 cm^{-1} (B species). In these complexes CO is bonded via a σ-bond only. Deeper reduction (773 K and above) led to the formation of V^{3+} sites, predominantly at the expense of the A species. These cations formed two kinds of carbonyl complexes (bands at 2197 and 2186 cm^{-1}) in which a weak π-back bonding is realized. As a result, the carbonyls were more stable than the V^{4+}–CO species and could be detected even at room temperature. The V^{3+} sites were fully oxidized by oxygen even at 85 K thus forming V^{4+} and V^{5+} species. At higher reoxidation temperatures (up to 373 K) the major part of the V^{4+} sites was also oxidized to V^{5+}. CO adsorption on VMgAPO-5 results in the formation of Mg^{2+}–CO species producing intense bands at 2187 and 2179 cm^{-1} which were superimposed on the V^{n+}–CO bands. For this reason the oxidation–reduction behavior of vanadium on this sample could not be studied in detail. It was found that some V^{4+} sites (producing a band at 2204 cm^{-1} at low temperature CO adsorption) were generated during the evacuation at 673 K. Deeper reduction with hydrogen created new sites (most probably V^{3+}) which were characterized by a carbonyl band at 2197 cm^{-1}. The nature of the V^{n+}–CO bonds as well as the effect of different factors on its strength are discussed. Some conclusions on the reduction–oxidation behavior of vanadium in the VAPO-5 and VMgAPO-5 are also presented.

1. INTRODUCTION

Supported vanadium oxides are known to be efficient catalysts in a number of selective catalytic oxidations and reductions, such as oxidation of methanol, methane and alkenes, oxidation and ammoxidation of aromatic hydrocarbons, and selective catalytic reduction of NO_x (1–5). The different catalytic behavior of supported vanadium catalysts is explained on the basis of the nature and distribution of the vanadium species, which are affected by the acid–base character of the support and the vanadium loading (6). Recently, it was reported that V-containing molecular sieves, such as V-silicalite, VAPO-5, and VMgAPO-5 materials, are highly selective for the oxidative dehydrogenation of ethane (7), propane (8, 9), and ethylbenzene (10). During the last years, great efforts have been made to determine the nature and the redox behavior of the vanadium species in the VAPO-5 materials (8, 11, 12).

Previously, different aluminophosphates containing vanadium (VAPO-5) or vanadium and magnesium (VMgAPO-5) have been prepared and characterized by different techniques (7, 8). These materials have shown high activity and selectivity in the oxidative dehydrogenation of propane (VAPO-5) and ethane (VMgPO-5). It was established that the major part of vanadium was incorporated in the structure. For the Mg-containing samples two kinds of Mg species were established: framework and extra-framework (charge-balancing cations) species. TPR of all samples displayed peaks with maxima at about 773 K. ESR revealed that calcined VAPO-5 contained negligible amounts of V^{4+}, whereas higher amounts of V^{4+} were observed for the magnesium-containing samples. Reduction generated V^{4+} in all samples and the highest concentration of these cations was detected for samples reduced at 673 K. For all samples reversible reduction–reoxidation was found.

It is of interest to study the VAPO-5 and VMgAPO-5 materials by infrared spectroscopy of adsorbed CO since the expected results could provide additional information on the properties of the samples and may be compared with the data obtained by other techniques. The infrared spectra of adsorbed CO provide information about the oxidation and coordination state of the surface cations, their location, etc. (13). Surprisingly, there are only a few available studies on CO adsorption on vanadium-containing samples (14–24). There is general agreement that V^{5+} ions do not form stable complexes with CO even at low temperature because of their high coordination saturation and the covalent character of the V–O bond (15–17). Most authors (15, 16,

---

[1] On leave from Instituto de Technologia Quimica, UPV-CSIC, Avda. Los Naranjos s/n, Valencia 46022, Spain.

[2] On leave from Institute of General and Inorganic Chemistry, Bulgarian Academy of Sciences, Sofia 1113, Bulgaria.

[3] To whom correspondence should be addressed at Institut für Physikdische Chemie, LMU, Bütenandtstrasse 5-13, Haus E, 81377 München, Germany.

0021-9517/99 $30.00

18, 19) proposed that V^{4+}–CO type carbonyls absorb in the range 2212–2180 cm^{-1}; these species are easy to remove by evacuation. Bands below 2192 cm^{-1} have been observed only after low-temperature CO adsorption (11). A number of authors (15, 18–22) have attributed the absorption region of 2190–2178 cm^{-1} to V^{3+}–CO carbonyls. These bands are difficult to eliminate by evacuation (23) which indicates some participation of a back π-bonding in the V^{3+}–CO bond.

The aim of this work is to study the surface carbonyls formed after CO adsorption on V-containing aluminophosphates subjected to different oxidation–reduction pretreatments. In order to monitor all sites and to prevent eventual reactive CO adsorption, the measurements were performed exclusively at low temperature, i.e., 85 K.

2. EXPERIMENTAL

2.1. Preparation of the Samples

The VAPO-5 and VMgAPO-5 materials were synthesized as described elsewhere (8). Briefly, $Al_2O_3/P_2O_5/V_2O_5/MgSO_4/H_2O/Et_3N$ gels with appropriate molar compositions were heated in teflon-lined stainless-steel autoclaves at 473 K for 16 h and then centrifuged, washed, and dried at 353 K. Finally, the samples were calcined at 823 K for 5 h in air. Highly crystalline materials were obtained with exclusively AFI structure in all the cases. Some characteristics of the samples as well as the sample notations that we shall use further on in the text are presented in Table 1.

2.2. Methods

IR spectroscopy studies were carried out with a Bruker IFS-66 apparatus at a spectral resolution of 1 cm^{-1} and collected 128 scans. Self-supporting wafers (ca. 10 mg cm^{-2}) were prepared from the sample powders and heated directly in the IR cell. The latter was connected with a vacuum/sorption apparatus with a residual pressure less than 10^{-3} Pa. Before the measurements all samples were activated for 1 h in a flow of oxygen at 673 K followed by 1 h evacuation at the same temperature. Reduction of the samples was carried out for 1 h in a flow of hydrogen at the respective temperature followed by evacuation at 673 K for 1 h. A specially constructed cell allowed the IR measurements to be performed at both ambient temperature and 85 K.

TABLE 1

Some Characteristics of the Investigated Samples

Sample	Vanadium content (wt%)[a]	Magnesium content (wt%)[a]	Crystallinity (%)[b]	S_{BET} (m^2 g^{-1})	Crystallite sizes (μm)[c]
VAPO-5	1.22	—	89	277	0.9–0.3
VMgAPO-5	0.53	2.68	71	185	12.5–8

[a] Vanadium and magnesium content in calcined samples, as wt% of V and Mg atoms.

[b] Crystallinity after calcination at 823 K, referenced to uncalcined $AlPO_4$-5.

[c] Obtained by SEM.

3. RESULTS

3.1. Sample VAPO-5

3.1.1. Hydroxyl coverage and adsorption of CO at ambient temperature. In the ν(OH) region there is only a weak band at 3675 cm^{-1} with a slight tailing toward lower frequencies. This band characterizes isolated OH groups. The reduction causes a slight decrease of the intensity of this band. This is attributed to the higher treatment temperatures during the reduction.

No carbonyl species were detected after CO adsorption at room temperature either on the oxidized sample or on the sample reduced at 673 K. However, on samples reduced at higher temperatures (773 and 883 K) adsorption of CO causes the appearance of one band with a very low intensity at ca. 2195 cm^{-1} having a shoulder at ca. 2185 cm^{-1}. Both bands slowly decrease with time and vanish at low equilibrium pressures. The intensity of the bands is higher when the prereduction temperature is higher.

3.1.2. Low-temperature CO adsorption on oxidized sample. Exposure of oxidized VAPO-5 at 85 K to CO (100 Pa equilibrium pressure) results in the appearance of a strong band at 2139 cm^{-1} which is typical for physically adsorbed CO (Fig. 1, spectrum a). In addition, a less intense band at 2169 cm^{-1} with a tail toward lower frequencies is also visible. In the ν(OH) region the hydroxyl band completely disappeared (the difference spectra showed a negative peak at 3678 cm^{-1}) and a new broad band at 3496 cm^{-1} emerged. Thus, the shift of the O–H stretching modes, $\Delta\nu$(OH), caused by H-bonded CO was −182 cm^{-1}.

A gradual decrease in the equilibrium pressure leads to a quick disappearance of the band assigned to physisorbed species (2139 cm^{-1}). Difference spectra have shown that this band has a pronounced high-frequency shoulder and a weaker one at low frequency. This complex contour of the band is due to hindered rotation modes (25). At lower pressures, the intensity of the band at 2169 cm^{-1} also decreases and the original spectrum of the surface OH groups is gradually restored. Hence, the band at 2169 cm^{-1} is attributed to CO H-bonded to surface hydroxyls (26). All bands are removed after 1 min evacuation at 85 K.

3.1.3. Low-temperature CO adsorption on sample reduced at 673 K. Adsorption of CO at 85 K on the 673-K reduced sample results again in the appearance of the bands due to physically adsorbed CO (2139 cm^{-1}) and CO H-bonded to the surface OH groups (2169 cm^{-1}) (Fig. 1, spectrum b). In this case, however, two more bands are observed at higher frequencies, their maxima being located at 2200 and 2194 cm^{-1}. These bands are readily observed at very low pressures, when all of the physically adsorbed CO and CO attached to OH groups is removed (Fig. 2). Both bands decrease in intensity under dynamic vacuum but it is the band at 2194 cm^{-1} that is more sensitive to evacuation. The 2200 cm^{-1} band is removed from the spectrum only after prolonged evacuation at 85 K. The fact that both bands were not detected on the oxidized sample as well as their nonsynchronous change in intensity permits us to assign them to CO adsorbed on two kinds of reduced V^{n+} sites. The low stability of the carbonyls implies that CO is bound to the cationic sites via a σ-bond only (13).

3.1.4. Low-temperature CO adsorption on sample reduced at 773 K. Adsorption of CO at 85 K on the sample reduced at 773 K leads to the same spectra in the 2180–2100 cm^{-1} region as those described above (Fig. 1, spectrum c). The only difference is that the band characterizing physically adsorbed CO is more intense. However, the differences in the higher frequency region (relative to the spectra recorded with the sample reduced at 673 K) are more important (see Fig. 3a). First, the band at 2194 cm^{-1} is much more intense, whereas the 2200 cm^{-1} band has lost some intensity. Second, a new, relatively intense band at 2186 cm^{-1} is clearly observed.

As in the cases described above, evacuation leads to fast disappearance of the 2139 and 2169 cm^{-1} bands. The next band that starts to vanish (Fig. 3b) is that at 2194 cm^{-1} followed by the bands at 2200 and 2186 cm^{-1}. A new band at 2197 cm^{-1} which is very resistant toward evacuation and which has been masked by the 2194 and 2200 cm^{-1} bands is now clearly visible (see Fig. 3a). After further evacuation the band at 2186 cm^{-1} disappears from the spectrum and the broad band at 2197 cm^{-1} is the principal one observed after prolonged evacuation.

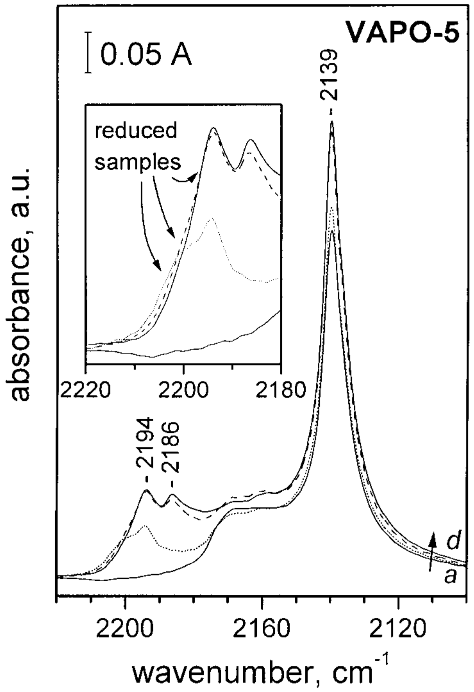

FIG. 1. FTIR spectra of CO (100 Pa equilibrium pressure) adsorbed at 85 K on VAPO-5 pretreated at different conditions. Oxidized sample (a), and samples reduced at 673 (b), 773 (c), and 873 K (d).

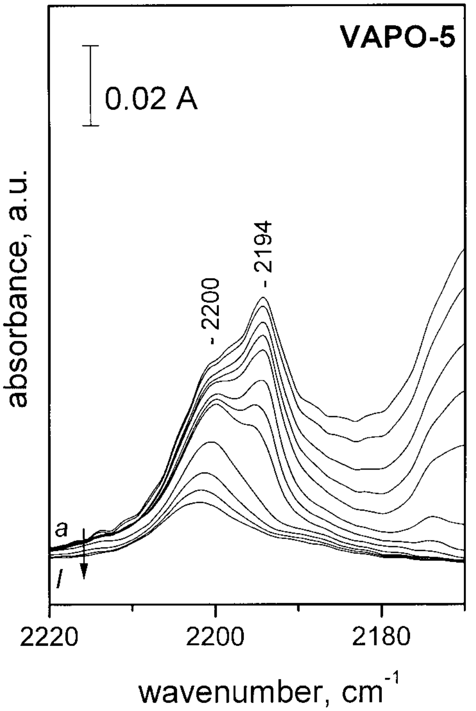

FIG. 2. FTIR spectra of CO adsorbed at 85 K on VAPO-5, prereduced at 673 K. Equilibrium pressure of 100 (a), 20 (b), and 10 (c) Pa CO, evacuation of the sample for short times (d–h), and time evolution of the spectra under dynamic vacuum (i–l).

Since the stretching frequency of CO adsorbed on a definite cation typically increases with the cation's Lewis acidity, it is evident that the 2186 cm^{-1} band cannot be attributed to another kind of σ-bonded V^{n+}–CO species. The somewhat higher stability of the respective carbonyls (compared to the V^{n+}–CO species) implies the formation of a weak π-back bonding, which suggests a lower oxidation state of the cation coordinating CO. Taking into account that the respective sites are created at higher reduction temperature only, we attribute the 2186 cm^{-1} band to V^{m+}–CO species, where $m < n$. The same considerations are valid for the band at 2197 cm^{-1} when comparing it with the 2200 cm^{-1} band.

3.1.5. Low-temperature CO adsorption on sample reduced at 873 K. The overall situation with this sample is similar to that with the sample reduced at 773 K. However, the bands at 2194 and 2186 cm^{-1} gained some intensity, whereas that at 2200 cm^{-1} disappeared (Fig. 4 and Fig. 5, spectrum a).

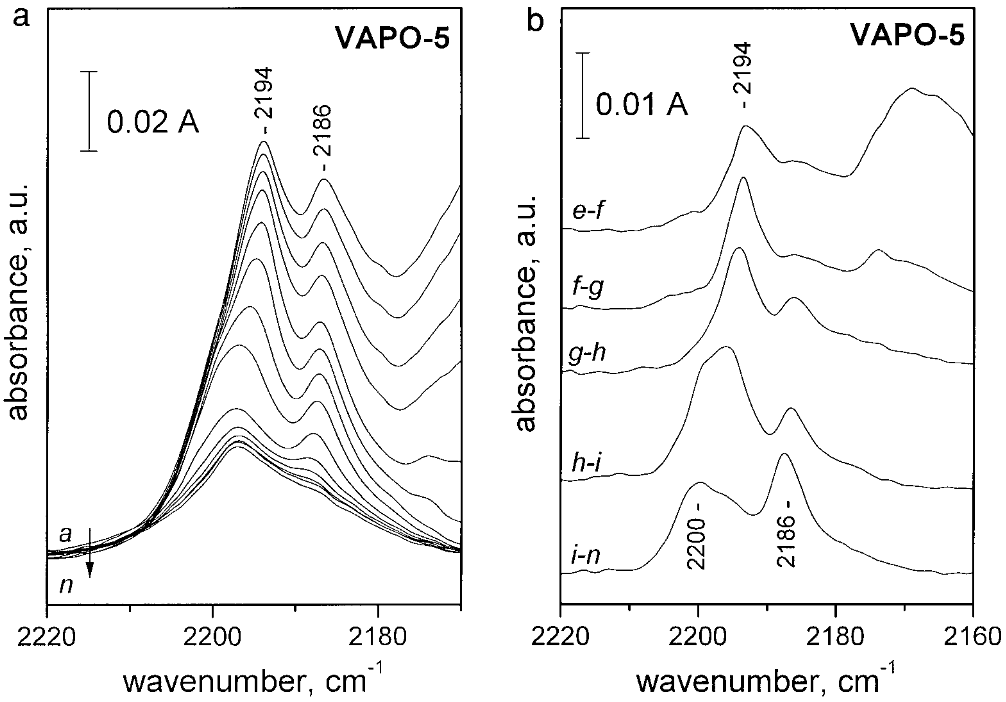

FIG. 3. (a) FTIR spectra of CO adsorbed at 85 K on VAPO-5, prereduced at 773 K. Equilibrium pressure of 100 (a), 20 (b), and 10 (c) Pa CO, evacuation of the sample for short times (d–h), and time evolution of the spectra under dynamic vacuum (i–n). (b) Difference spectra from (a).

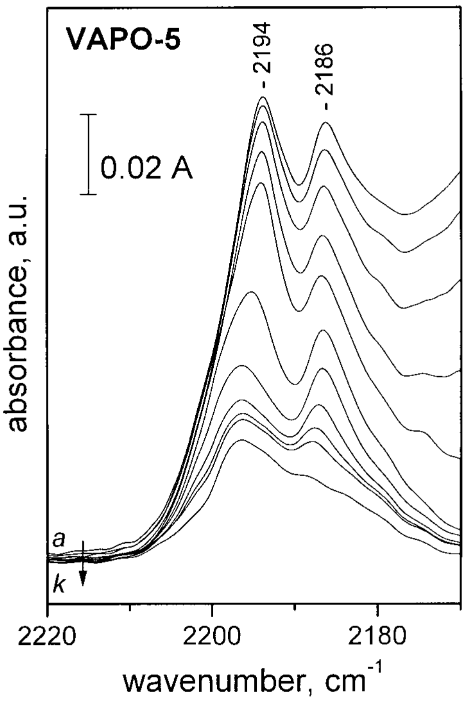

FIG. 4. FTIR spectra of CO adsorbed at 85 K on VAPO-5, prereduced at 873 K. Equilibrium pressure of 100 (a) and 30 Pa CO, evacuation of the sample for short times (c–d), and time evolution of the spectra under dynamic vacuum (e–k).

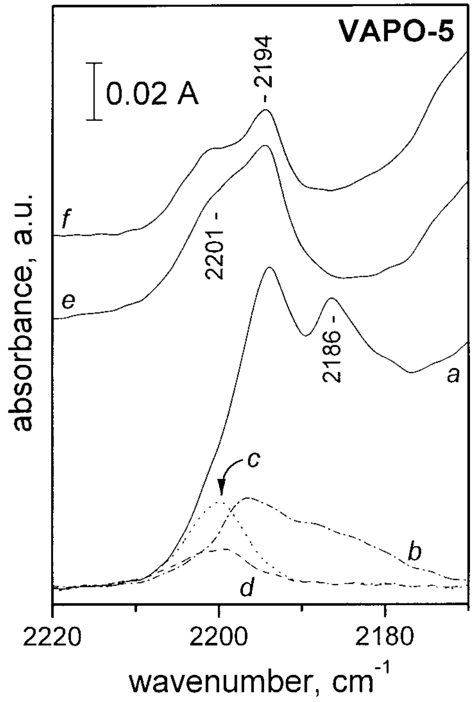

FIG. 5. FTIR spectra of CO adsorbed at 85 K on VAPO-5. Sample reduced at 873 K after adsorption of CO (100 Pa) (a), followed by evacuation at 85 K (b), subsequent introduction of 100 Pa O_2 (c), and evacuation (d), followed by introduction of 100 Pa CO (e). The sample was heated for 15 min in 10 kPa O_2, evacuated, cooled to 85 K, and subjected to 100 Pa of CO (f).

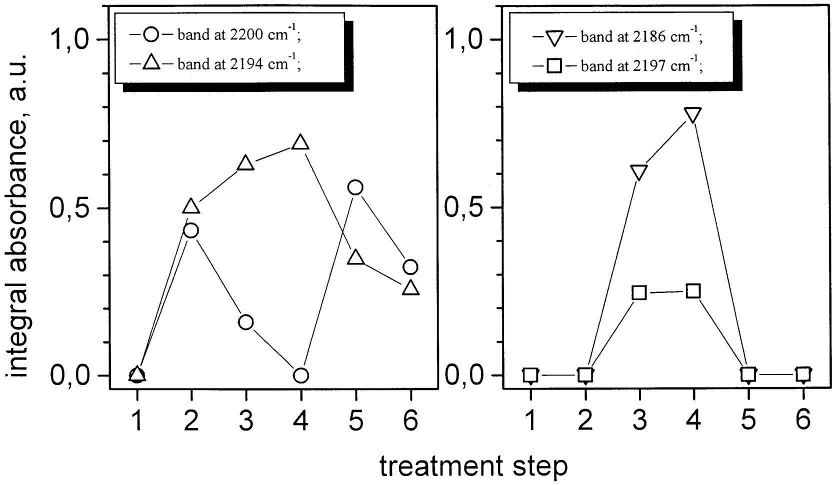

FIG. 6. Variation of the intensity of the different vanadium carbonyl bands (100 Pa CO at 85 K) depending on the pretreatment of the VAPO-5. Oxidized sample (1); sample reduced at 673 (2), 773 (3), and 873 K (4), and reoxidized at 85 (5) and 293 K (6).

During the evacuation it is again the 2194 cm^{-1} band that disappears first, followed by the band at 2186 cm^{-1}. A careful inspection of the different spectra indicates that a small fraction of sites characterized by a carbonyl band at 2200 cm^{-1} are generated with time. This is most probably caused by an oxidation of some V^{m+} sites to V^{n+} by minute amounts of oxygen entering into the IR cell, or by reaction of V^{m+} sites with V^{5+} giving V^{n+}.

3.1.6. Low-temperature CO adsorption on reoxidized sample. It was of interest to test the stability of the reduced vanadium species in the presence of oxygen. Therefore, the sample reduced at 873 K was evacuated (a residual CO band at 2197 cm^{-1} with a shoulder at 2186 cm^{-1} are characteristic of the spectrum; see Fig. 5, spectrum b) and then exposed to 20 Pa oxygen at 85 K. This caused the disappearance of the bands at 2197 and 2186 cm^{-1} and the appearance of a band at 2200 cm^{-1} which is not stable toward evacuation (Fig. 5, spectra c, d). To monitor all of the Lewis acid sites existing on the surface after this treatment, oxygen was evacuated and 100 Pa CO introduced to the sample (Fig. 5, spectrum e). It is evident that the species characterized by the band at 2187 cm^{-1} have disappeared. The deconvolution spectra (see also Fig. 6, step 5) show that the band at 2197 cm^{-1} which is stable against evacuation also vanished, and only two carbonyl bands, at 2194 and 2200 cm^{-1}, are detected.

When the re-oxidation was performed at a higher temperature, namely 373 K, subsequent adsorption of CO (Fig. 5, spectrum f) reveals an additional decrease of the population of the sites characterized by bands at 2194 and 2200 cm^{-1}. The variations of the intensities of the different bands at various oxidation–reduction steps are shown in Fig. 6.

3.2. Sample VMgAPO-5

3.2.1. Hydroxyl coverage and adsorption of CO at room temperature. The hydroxyl coverage of this sample is similar to that of VAPO-5. In the ν(OH) region one band characteristic of isolated OH groups is detected at 3677 cm^{-1}. Here again the reduction causes an decrease in the intensity of the OH band.

Adsorption of CO at ambient temperature on the sample, either oxidized or reduced at 673 K, does not lead to formation of surface carbonyl species. A weak band at about 2198 cm^{-1} was observed with the samples reduced at 773 and 873 K. Note, however, that its position cannot be exactly determined because of its very low intensity.

3.2.2. Low-temperature CO adsorption on an oxidized sample. Adsorption of CO at 85 K on the VMgAPO-5 results in a spectrum which is definitely more complex than that recorded for the VAPO-5 sample. A strong band at 2139 cm^{-1} having a pronounced low-frequency shoulder is due to physically adsorbed CO (Fig. 7). The difference spectra reveal the existence of one high frequency shoulder as well. The band caused by CO H-bonded to surface hydroxyls is observed at 2170–2168 cm^{-1}. Simultaneously with the appearance of this band a red shift of the OH stretching mode from 3677 to 3525 cm^{-1} ($\Delta\nu(\text{OH}) \approx -150$ cm^{-1}) is observed.

Three more bands are detected at higher frequencies (Fig. 8, spectrum a): namely, an intense band at 2179 cm^{-1} and two weaker ones with maxima at 2204 and 2187 cm^{-1}. It is the band at 2179 cm^{-1} that is most sensitive to evacuation; it rapidly decreases as the equilibrium CO pressure decreases and it slightly shifts at low coverages toward higher frequencies. The next band disappearing after evacuation is that at 2187 cm^{-1}. The 2204 cm^{-1} band is highly resistant toward evacuation at this temperature.

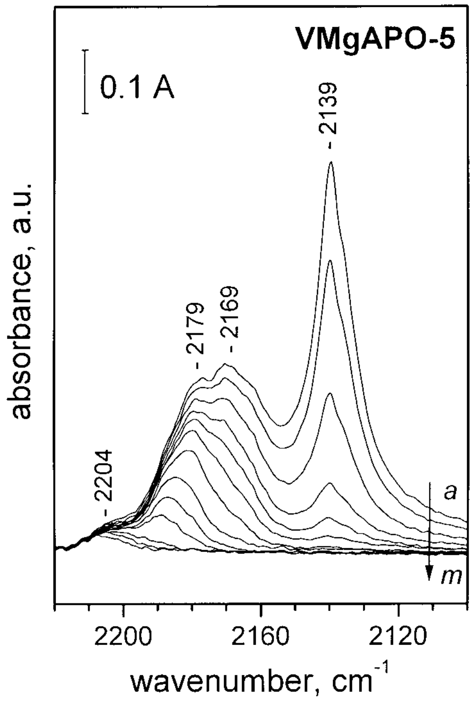

FIG. 7. FTIR spectra of CO adsorbed at 85 K on oxidized VMgAPO-5. Equilibrium pressure of 2 (a), 0.4 (b), 0.2 (c), and 0.1 (d) hPa CO; evacuation of the sample for increasing times (e–j) and under dynamic vacuum (k–m).

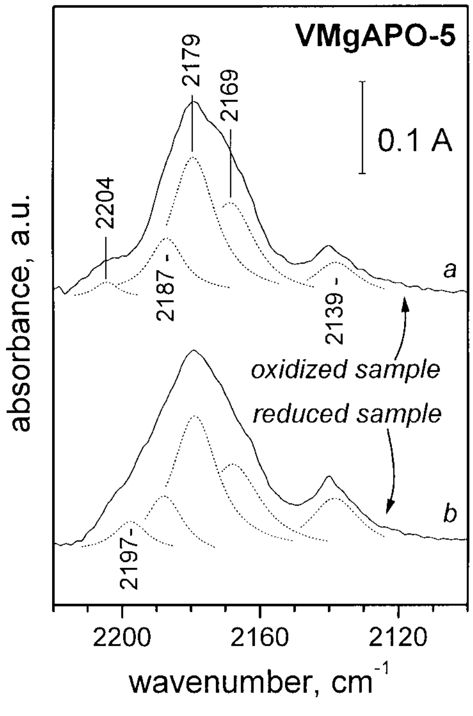

FIG. 8. FTIR spectra of CO adsorbed at 85 K on VMgAPO-5 oxidized (a) and reduced at 873 K (b). The spectra are taken after a short evacuation of CO.

3.2.3. Low-temperature CO adsorption on reduced samples. The spectra of CO adsorbed on the reduced VMgAPO-5 differ from those recorded for the oxidized samples mainly in the 2210–2160 cm^{-1} region. With increasing temperature of reduction the band at 2204 cm^{-1} decreases and is not observed on the sample reduced at 873 K (Fig. 8, spectrum b). Simultaneously, a new band at 2197 cm^{-1} develops. Although highly resistant toward evacuation, this band disappears from the spectrum after prolonged pumping. The band at 2169 cm^{-1} is reduced in intensity which is consistent with the lower hydroxyl coverage of the reduced samples. It seems that the intensities of the bands at 2179 and 2187 cm^{-1} do not depend on the sample pretreatment, which suggests that they are not due to V^{n+}–CO species. According to data from the literature (27) we assign these bands to two kinds of Mg^{2+}–CO carbonyls.

4. DISCUSSION

4.1. Sample VAPO-5

The positive charge of the cations and the strength of the σ-donor bond with CO decreases in the sequence $V^{4+} > V^{3+} > V^{2+}$ and would thus lead to a decrease in absorption frequencies and the stability of carbonyls. Due to their high charge, the V^{4+} ions cannot undergo π-back bonding with adsorbed CO; i.e., the carbonyl complexes of V^{4+} are characterized by a σ-donor bond only. The charge of the V^{3+} ions is still high and the d-electron density is low, so that the formation of a π-back bond is expected to be weak and that of V^{3+} carbonyls to be unstable and to decompose during evacuation at ambient temperature. Strengthening of the V–CO bond due to π-back donation can be expected with V^{2+} cations because of their low charge. This would cause both a decrease in absorption frequency and a strengthening of the vanadium–carbon bond in the V^{2+}–CO complexes.

Since the results obtained in this study with VAPO-5 are more comprehensible, the discussion about the different vanadium carbonyls will be based, preferentially, on this sample. Our results are in agreement with the general view that V^{5+} species do not form carbonyl complexes. CO adsorption on VAPO-5 reduced at 673 K produces two bands (at 2200 and 2194 cm^{-1}) which can be assigned to V^{4+} carbonyls. These assignments are in agreement with the spectral region (2212–2180 cm^{-1}) at which different authors (15, 16, 18, 19) have proposed V^{4+}–CO species to absorb. This is also consistent with ESR data indicating a high concentration of V^{4+} in samples thus treated (8). The stability of these carbonyls is low and they can be detected at low temperatures only. This is in agreement with the above proposed considerations and indicates that in this case only a σ-bond is formed between V^{4+} and CO. As expected, the species characterized by a band at higher frequency (2200 cm^{-1}) form stronger σ-bonds and are more stable. It is known that the molar extinction coefficient of the C–O stretching mode does not strongly depend on the σ-bond strength (28). Hence, in this case, the intensity of the IR bands can be used for an estimation of the relative concentration of the respective species. Thus, the carbonyls producing a band at 2200 cm^{-1} are of lower concentration.

Deeper reduction of the samples creates two new vanadium sites, the respective carbonyl bands being located at 2197 and 2186 cm^{-1}. These bands are highly resistant toward evacuation at 85 K and can be detected (although with very low intensities) even at room temperature. Let us consider the 2194–2186 cm^{-1} pair of bands. The 2186 cm^{-1} band has a lower frequency, but the respective species are more stable. However, with cations forming predominantly σ-bonds with CO, the higher the stability of the carbonyls, the higher their stretching frequency. This implies that the two bands cannot be assigned to carbonyls of vanadium cations having the same oxidation states. The higher stability and the lower frequency of the 2186 cm^{-1} band species suggests some back π-donation. Hence, this band is due to carbonyls formed with the participation of vanadium ions in an oxidation state lower than 4. Thus, the band at 2186 cm^{-1} is attributed to V^{3+}–CO species.

Analogous considerations hold when one compares the pairs of bands at 2200 and 2197 cm^{-1}. Hence, the band at 2197 cm^{-1} may be assigned to another kind of V^{3+}–CO species. The higher stability and the higher frequency of the 2197 cm^{-1} species relative to those of the species characterized by a band at 2186 cm^{-1} indicates that, in the former case, the σ-bond between V^{3+} and CO is stronger. Another confirmation of the assignment of the 2197 and 2186 cm^{-1} bands to V^{3+}–CO species is their disappearance after oxidation of the sample even at 85 K. Note that no reliable conclusions about the relative concentration of the V^{3+} sites can be made in this case since the formation of π-back bonding enhances the molar extinction coefficient of CO.

The results obtained demonstrate that the spectral regions of V^{4+}–CO and V^{3+}–CO compounds superimpose. Hence, to distinguish between both kinds of species, one has to consider, in addition to the stretching frequencies, other factors such as stability of the species and their ease of oxidation.

Our result evidenced two kinds (A and B) of V^{4+} sites on reduced VAPO-5 which manifest different redox behavior. The A species are of lower concentration. They are easily reduced to V^{3+} at temperatures higher than 673 K and disappear completely after 873 K reduction. On the contrary, the concentration of the B species increases with the reduction temperature at least up to 873 K. At low temperature and in the presence of oxygen the V^{4+} A species are generated from V^{3+}, whereas oxidation of the B species to V^{5+} evidently occurs even at 85 K (see Fig. 7, step 5). Thus, it may be concluded that a higher oxidation state is more typical for the vanadium cations corresponding to B species.

One of the possible assignments of the A and B species is to extra-framework and to framework vanadium, respectively. However, the amount of extra-framework vanadium on our VAPO-5 sample is too low to produce carbonyl bands so intense as observed after CO adsorption (8). For that reason we are of the opinion that both kinds of species arise from a different incorporation mechanism of vanadium in the framework of $AlPO_4$-5 structure, i.e., in positions of Al^{3+} or P^{5+}.

Unfortunately, we cannot give an exact interpretation of the two kinds of V^{3+}–CO species. One may infer that the A species (V^{4+} cations detected by a band at 2200 cm^{-1}), being stronger Lewis acids, could generate V^{3+} cations after reduction which are characterized by a stronger acidity (CO band at 2196 cm^{-1}). Accordingly, the 2194 cm^{-1} species should produce V^{3+} cations characterized by carbonyls detected at 2186 cm^{-1}. However, our results support another possibility, i.e., both kinds of V^{3+} ions are produced by reduction of the A-type V^{4+} species.

The created V^{3+} cations are strongly reducing species and react readily with oxygen even at 85 K, thus producing V^{4+}. Based on the spectra of adsorbed CO, we cannot draw any conclusions on a direct oxidation of some of V^{3+} to V^{5+}. It is evident, however, that at higher temperature of re-oxidation, namely at 373 K, a significant part of V^{4+} is converted into V^{5+} species. Finally, the fact that the reduction–oxidation treatments do not affect the background spectrum of the sample implies that, in general, the structure of VAPO-5 is preserved during the experiments.

It is of interest to discuss the properties of the surface hydroxyl groups. The O–H stretching frequency of the isolated hydroxyl groups on our sample (3675 cm^{-1}) is close to the band position of both V–OH (29) and P–OH (30) groups. An additional criterion that can be involved for a correct assignment is the acidity of the hydroxyls. In general, the P–OH groups are expected to be more acidic than the V–OH ones. According to literature data (30) P–OH groups on phosphated zirconia manifest a red shift of $-135 \div -175$ cm^{-1} after low-temperature CO adsorption. In the present case we have measured a similar shift, i.e., -182 cm^{-1}. This allows us to assign the isolated OH groups on the VAPO-5 sample to P–OH hydroxyls.

4.2. *Sample VMgAPO-5*

The stretching frequency of the OH groups on the VMgAPO-5 is similar to that recordered for VAPO-5. In addition, the acidity of both kinds of hydroxyls, as measured by low-temperature CO adsorption, is also similar. Thus, we conclude that the surface hydroxyls on the VMgAPO-5 samples represent isolated P–OH groups.

The low temperature CO adsorption on VMgAPO-5 resulted in the appearance of two Mg^{2+}–CO bands at 2187 and 2179 cm^{-1} whose intensities do not depend on the sample pretreatment. We tentatively assign the band at 2187 cm^{-1} to species formed on extra-framework Mg^{2+} cations (which is consistent with their lower concentration) and the band at 2179 cm^{-1} to framework Mg^{2+}. The existence of two kinds of Mg^{2+} in the samples was earlier proved by independent techniques (31).

Contrary to the results obtained for VAPO-5, the vacuum treatment of the VMgAPO-5 leads to the creation of some V^{4+} species (carbonyl band at 2204 cm^{-1}). Their low concentration suggests that they are formed via the autoreduction of extra-framework vanadium. The existence of V^{4+} in these samples after calcination treatment is consistent with earlier observations by other techniques (7). Deeper reduction leads to the disappearance of this band and a new band at 2197 cm^{-1} emerges. This behavior suggests the latter band is due to V^{3+}–CO species. Unfrotunately, due to the strong intensity of the Mg^{2+}–CO bands, it was not possible to carry out a detailed analysis of the V^{n+}–CO bands produced on the VMgAPO-5 sample.

5. CONCLUSIONS

- Mild reduction of VAPO-5 with hydrogen (673 K) generates two kinds of V^{4+} sites which can be detected by CO only at low temperature by bands at 2200 and 2194 cm^{-1}. In these complexes CO is coordinated via a σ-donor bond.
- Deeper reduction of VAPO-5 with hydrogen (773 K and above) leads to the formation of V^{3+} sites. These cations form two kinds of carbonyl complexes (bands at 2197 and 2186 cm^{-1}) in which a weak π-back bonding is realized. As a result, the V^{3+}–CO carbonyls are more stable than the V^{4+}–CO species and can be detected at room temperature.
- The V^{3+} sites in VAPO-5 are fully oxidized by oxygen even at 85 K thus forming V^{4+} and eventually V^{5+} species. At higher reoxidation temperatures (up to 373 K) the major part of the V^{4+} sites is also oxidized to V^{5+}.
- Some V^{4+} sites are created on VMgAPO-5 during the evacuation of the samples at 673 K. These sites can be monitored by CO only at low temperature by a band at 2204 cm^{-1}. Deeper reduction with hydrogen creates a new kind of sites (most probably V^{3+}) which is characterized by a carbonyl band at 2197 cm^{-1}.
- The spectral regions in which V^{4+}–CO (at least 2204–2194 cm^{-1}) and V^{3+}–CO (2197–2186 cm^{-1}) species are detected, superimpose. Hence, other factors (stability, reactivity toward oxygen) have to be considered in addition to the carbonyl stretching frequency to distinguish both kinds of species.

ACKNOWLEDGMENTS

This work was financially supported by the Deutsche Forschungggemeinschaft (SFB 338) and the Fondes der Chemischen Industrie. K.H. acknowledges a fellowship from the Alexander von Humboldt-Stiftung, P.C. a grant from the Fonds der Chemischen Industrie.

REFERENCES

1. Centi, G., Perathoner, S., and Trifiró, F., *Res. Chem. Intermed.* **15**, 49 (1991).
2. Kung, H. H., *Ind. Eng. Chem. Prod. Res. Dev.* **25**, 171 (1986).
3. Dadyburjor, D. B., Jewur, S. S., and Ruckenstein, E., *Catal. Rev. Sci. Eng.* **19**, 293 (1979).
4. Wainwright, M. S., and Foster, N. F., *Catal. Rev. Sci. Eng.* **19**, 211 (1979).
5. Cavani, F., and Trifiró, F., *Appl. Catal. A* **133**, 219 (1995).
6. Blasco, T., López Nieto, J. M., Dejoz, A., and Vázquez, M. I., *J. Catal.* **157**, 271 (1995).
7. Concepción, P., López Nieto, J. M., Mifsud, A., and Pérez Pariente, J., *Appl. Catal. A* **151**, 373 (1997).
8. Blasco, T., Concepción, P., López Nieto, J. M., and Pérez Pariente, J., *J. Catal.* **152**, 1 (1995).
9. Bellussi, G., Centi, G., Perathoner, S., and Trifiró, F., *in* "Catalytic Selective Oxidation," A. C. S. Symp. Series, Vol. 523, p. 281. Am. Chem. Soc., Washington, DC, 1993.
10. Hong, S. B., Hwang, B. W., Yeom, Y., Kim, S. J., and Uh, Y. S., *in* "Chemistry of Microporous Crystals" (T. Uni, S. Namba, and T. Tatsumi, Eds.), Elsevier, Amsterdam, *Stud. Surf. Sci. Catal.* **60**, 179 (1991).
11. Wechuysen, B. M., Vannijvel, I. P., and Schoonheydt, R. A., *Zeolites* **15**, 482 (1995).
12. Rigutto, M. S., and van Bekkum, H., *J. Mol. Catal.* **81**, 77 (1993).
13. Knözinges, H., in "Handbook of Heterogeneous Catalysis" (G. Ertl, H. Knözinger, and I. Weitkamp, Eds.), p. 707, Wiley-VCH, Weinheim, 1997.
14. Davydov, A., Budneva, A., and Maksimov, N. G., *React. Kinet. Catal. Lett.* **20**, 93 (1982).
15. Davydov, A., and Shepotko, M., *Teor. Eksper. Khim.* **26**, 505 (1990).
16. Sobalic, Z., Kozlowski, R., and Haber, J., *J. Catal.* **127**, 665 (1991).
17. Jonson, B., Rebenstorf, B., Larsson, R., and Andersson, S. L. T., *J. Chem. Soc. Faraday Trans. 1* **84**, 1897 (1988).
18. Gerasimov, S., and Filimonov, V., *Kinet. Katal.* **22**, 469 (1981).
19. Jonson, B., Rebenstorf, B., and Larsson, R., *Acta Chem. Scand. A* **42**, 156 (1988).
20. Jonson, B., Rebenstorf, B., Larsson, R., and Andersson, S. L. T., *J. Chem. Soc. Faraday Trans. 1* **84**, 3363 (1988).
21. Rebenstorf, B., Berglund, M., Lykvist, R., and Larsson, R., *Z. Phys. Chem.* **126**, 595 (1981).
22. Maschenko, A., Kou, M., Shvetz, V., and Kazanskii, V., *Teor. Eksp. Khim.* **8**, 801 (1972).
23. Busca, G., Ramis, G., and Lorenzelli, V., *J. Mol. Catal.* **50**, 231 (1989).
24. Jonson, B., Rebenstorf, B., Larsson, R., Andersson, S. L. T., and Lundin, S. T., *J. Chem. Soc. Faraday Trans. 1* **82**, 767 (1986).
25. Morterra, C., Ghiotti, G., Boccuzzi, F., and Coluccia, S., *J. Catal.* **51**, 299 (1978).
26. Zaki, M., and Knözinger, H., *Mater. Chem. Phys.* **17**, 281 (1987).
27. Coluccia, S., Baricco, M., Marchese, L., Martra, G., and Zecchina, A., *Spectrochim. Acta. A* **49**, 1289 (1993).
28. Angell, C., and Schaffer, P., *J. Phys. Chem.* **70**, 1413 (1966).
29. Kantcheva, M., Hadjiivanov, K., and Klissurski, D., *J. Catal.* **134**, 299 (1992).
30. Spielbauer, D., Mekhemer, G. A. H., Riemer, T., Zaki, M., and Knözinger, H., *J. Phys. Chem. B* **101**, 4681 (1997).
31. Concepción, P., Ph.D. thesis, Instituto de Technologia Quimica, UPV, Valencia, 1996.